8.5.4 Aharonov-Bohm ring

As an application of S-matrix, we consider the transmission coefficient of an Aharonov-Bohm (AB) ring. The channel configuration is shown in Fig. 8.19(a). We write the S-matrix for the two junctoins with three channels as [*1]

$$S_t = \begin{pmatrix} 0 & -1/\sqrt{2} & -1/\sqrt{2} \\ -1/\sqrt{2} & 1/2 & -1/2 \\ -1/\sqrt{2} & -1/2 & 1/2 \end{pmatrix}. \tag{8.51}$$

The AB phase is taken into account by inserting

$$S_{\mathrm{AB}} = \begin{pmatrix} 0 & e^{i\theta_{\mathrm{AB}}} \\ e^{-i\theta_{\mathrm{AB}}} & 0 \end{pmatrix}, \qquad \theta \equiv 2\pi\frac{\phi}{\phi_0} = \frac{e}{\hbar}\phi \ \ (\phi \text{ is the flux piercing the ring}) \tag{8.52}$$

into one of the parallel paths. We insert the S-matrix

$$S_{\mathrm{w}} = \begin{pmatrix} 0 & e^{i\theta_0} \\ e^{i\theta_0} & 0 \end{pmatrix} \tag{8.53}$$

into the counter arm to express the phase difference between the two paths. The phase shift θ_0 from the path difference does not depend on the direction of the propagation while the sign of θ_{AB} is inverted with inversion of propagation. The Onsager reciprocity (8.18) is kept with these mathematical settings.

From the total S-matrix, the complex transmission coefficient of the ring is obtained as[3]

$$t = \frac{4\sin\theta_0}{1 + e^{i\theta_{\mathrm{AB}}}\left(e^{i\theta_{\mathrm{AB}}} + e^{i\theta_0} - 3e^{-i\theta_0}\right)}. \tag{8.54}$$

The transmission coefficient $T = |t|^2$ shows AB oscillation of the period ϕ_0 in ϕ (the magnetic flux piercing the ring). T also oscillates versus θ_0 with the period of 2π. $|t|^2$ is symmatric for $\phi = 0$, which is due to the reciprocity induced on (8.54) by the Onsager reciprocity introduced into S-matrix (8.52).

The phase of the oscillation with period ϕ_0 varies on θ_0 as a rectangular wave with amplitude π. The amplitude of the oscillation disappears around the phase jumps, which does not mean the disappearance of the magnetoresistance oscillation and the $\phi_0/2$ period and higher frequency components increase in the amplitudes. As above, the ϕ_0-oscillation only takes the phase offset of 0 or π, which property is called "phase rigidity[4]." The phase rigidity means that we cannot detect the phase shift over the quantum dot inserted into one of the arms of an AB ring[*2] .

8.6 Qauntum transport and particle statistics

As a transport phenomenon in a semiconductor, the transport of electrons (charge and spin) is often considered, but some quasiparticles baring transport behave differently from electrons. We will have a look how we apply the quantum transport theory (or not apply).

[*1] This form is frequently adopted though it is completely symmetric and a bit special in that sense.

[*2] If we consider multiple conductance channels and also restrict the region of magnetic field, the phase looks smoothly changes with flux[5] though this does not mean the breaking of the Onsager reciprocity.

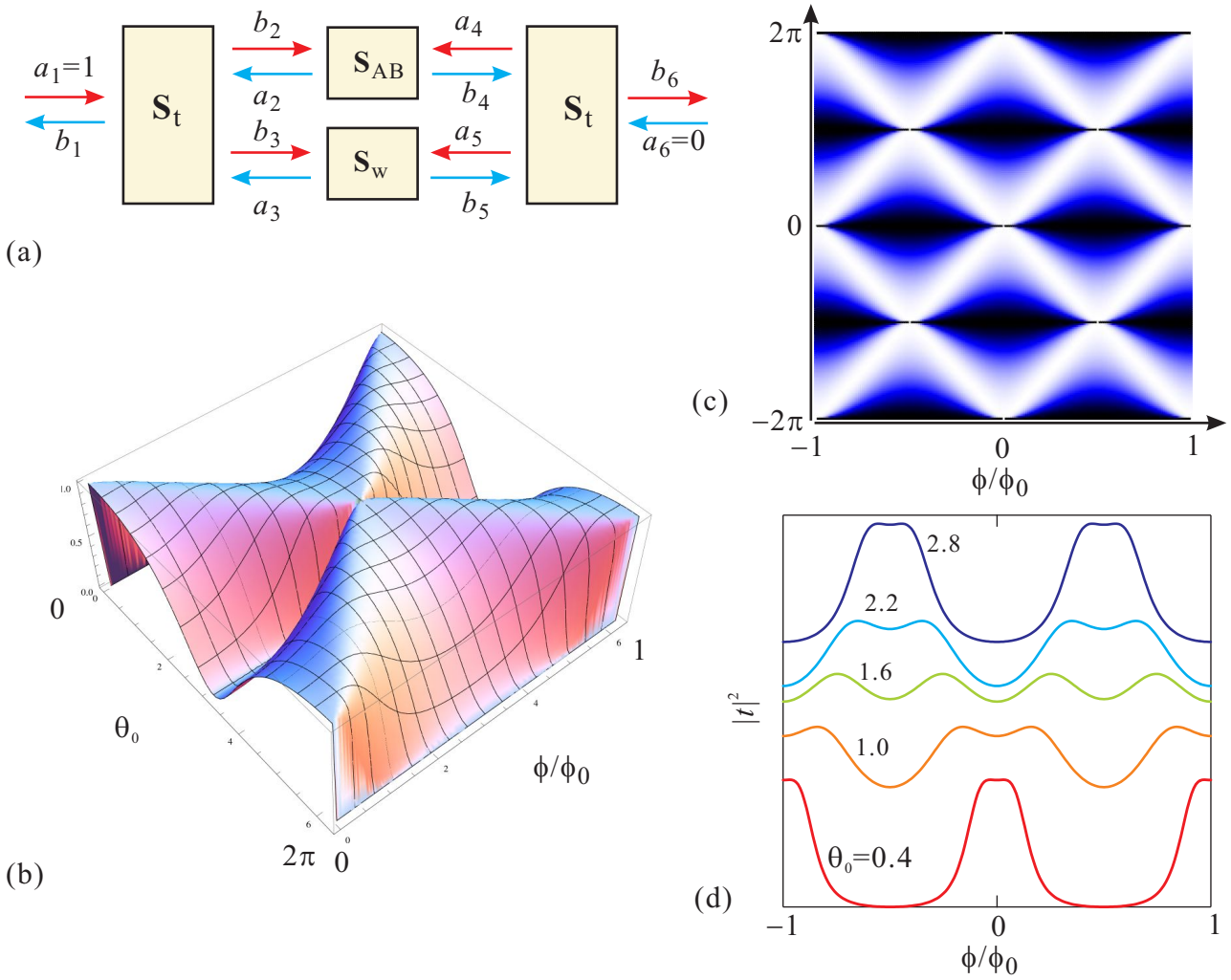

Fig. 8.19 (a) S-matrix modeling of an AB ring. (b) The transmission coefficient of the AB ring $|t|^2$ is plotted (surface plot) as a function of the phase shift from the path difference (θ_0) and the magnetic flux piercing the ring ϕ/ϕ_0. (c) Color plot of the same calculation over a bit wider region. (d) The same transmission coefficient as a function of ϕ/ϕ_0 with θ_0 as a parameter. The AB oscillation of period ϕ_0 once disappears around $\theta_0 = 1.6$ and then the reverted oscillation, that is, with π-shift in the phase appears.

8.6.1 Bunching, anti-bunching

In the previous section, we have introduced the Landauer formula to treat the electric conduction in semiconductor quantum structures. In the discussion, we assumed the transport of electrons and used the unit charge and the Fermi distribution in the derivation. And the conductance quantization is derived from the anti-bunching of fermions on quantum wires. On the other hand, in order to calculate the transmission coefficient T_{ij}, we have introduced T-matrices and S-matrices scheme. These are only to calculate the transmission and reflection of waves without the relation to the particle statistics. Hence the method should be applicable regardless of particle statistics.

Let us have a look on bunching and anti-bunching properties. The wavefunction for identical two particls is in real coordinate representation as

$$\psi(\boldsymbol{r}_1, \boldsymbol{r}_2) = \frac{1}{\sqrt{2}}[\phi_1(\boldsymbol{r}_1)\phi_2(\boldsymbol{r}_2) \pm \phi_1(\boldsymbol{r}_2)\phi_2(\boldsymbol{r}_1)]. \tag{8.55}$$

In the double sign, $+$ corresponds to bosons, and $-$ to fermions.

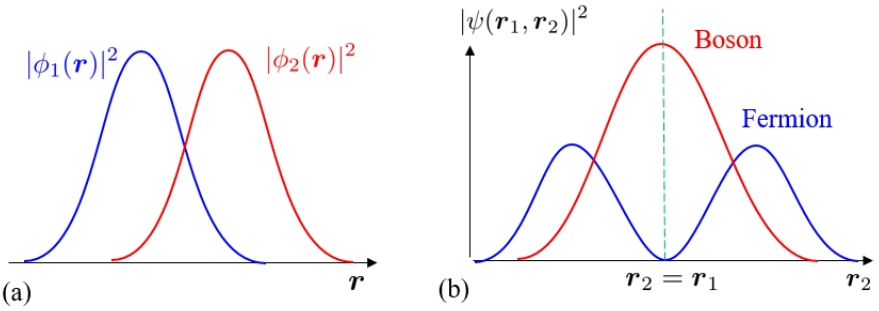

Fig. 8.20 (a) Schematic probability densities in coordinate representation $|\phi_1(\boldsymbol{r})|^2$, $|\phi_2(\boldsymbol{r})|^2$ of one-particle wavefunctions. The two wavefunctions have a partial overlap. (b) In the case of (a), the spatial probability density of particle 2 is plotted as a function of coordinate $\boldsymbol{r}_2$ with taking the position of the particle 1 $\boldsymbol{r}_1$ as the origin in the two-particle wavefunction ϕ in (8.55).

As shown in Fig. 8.20(a), we consider gaussian shaped wavefunctions $\phi_{1,2}(\boldsymbol{r})$ with partial overlap. Figure 8.20(b) shows the probability density of the two-particle wavefunction versus the relative position. As we can easily see by putting $\boldsymbol{r}_2 = \boldsymbol{r}_1$, the probability densities are

$$|\psi(\boldsymbol{r}_1,\boldsymbol{r}_1)|^2 = \begin{cases} 2|\phi_1(\boldsymbol{r}_1)|^2|\phi_2(\boldsymbol{r}_1)|^2 & \text{(boson)}, \\ 0 & \text{(fermion)}. \end{cases} \tag{8.56}$$

That is, in the case of bosons, the probability density is twice the case of single particle while in the case of fermions the density is zero. This means that the **bunching** occurs for bosons while the **anti-bunching** occurs for fermions.

The discussion of (8.3)∼(8.5), which leads to the Landauer formula can be understood in this context of anti-bunching. That is, the difference in the chemical potentials of two electron reservoirs, eV is the energy window to be used to form the wave packets of elctrons *i.e.*, $\Delta E \sim eV$. The time for such a wave packet to go through a point in the real space is, from the uncertainty relation, $\Delta t = h/\Delta E = h/eV$. From the anti-bunching property or Fermi statistics, a single wave packet can accomodate a single elecrtron (if the spin degree of freedom is taken into account, two electrons). Then the current flowing though the one-dimensional system is $J = e/\Delta t = (e^2/h)V$ (with spin freedom, $(2e^2/h)V$), which results in the same conclustion in the previous section.

The above discussion is the same calculation of that done in the k-space though it gives an important insight of the flow of electrons on quantum wires. When the conductance is quantized in such a quantum wire, the electrons flow with the time interval of h/eV. As is describe in the shot noise section of Appendix 8A, the current flow is approximated as a periodic series of delta-functions and the shot noise disappears. In the Landauer's discussion, the conductance quantization is the consequence of the fermion's anti-bunching property and the above consideration means that can be experimentally confirmed through shot noise measurement.

We expand the above to quantum wires with transmission coefficients $\mathcal{T}$ less than 1 to get $G = \mathcal{T}G_{\rm q}$. In this case, there appear free spaces between the wave packet due to the electron reflection and the packing of electrons becomes stocastic to some degree. This states can be viewed as follows. A perfectly ordered series of wave packets are occupied by electrons with probability $\mathcal{T}$, by holes with probability $1-\mathcal{T}$. Identical electrons (also holes) cannot be distinguished and the number of cases for vacancies, *i.e.* the degree of randomness is proportional to $\mathcal{T}(1-\mathcal{T})$. In the limit $\mathcal{T} \to 0$, this goes to Eq. (8A.3) and with using the relation $J = 2\mathcal{T}G_{\rm q}V$ for voltage V, the noise power spectrum is given as[**?**]

$$S \equiv \frac{\langle(\delta J)^2\rangle}{\Delta f} = 2e\frac{2e^2}{h}V\mathcal{T}(1-\mathcal{T}). \tag{8.57}$$

The above S is suppressed from $S_{\rm Poisson}$ in Eq. (8A.3) by factor $1-\mathcal{T}$. Generally, we refer to **Fano factor** as the ratio of variance to the average. In the present case that corresponds to the ratio of the shot noise to the Poisson noise and is $1-\mathcal{T}$.

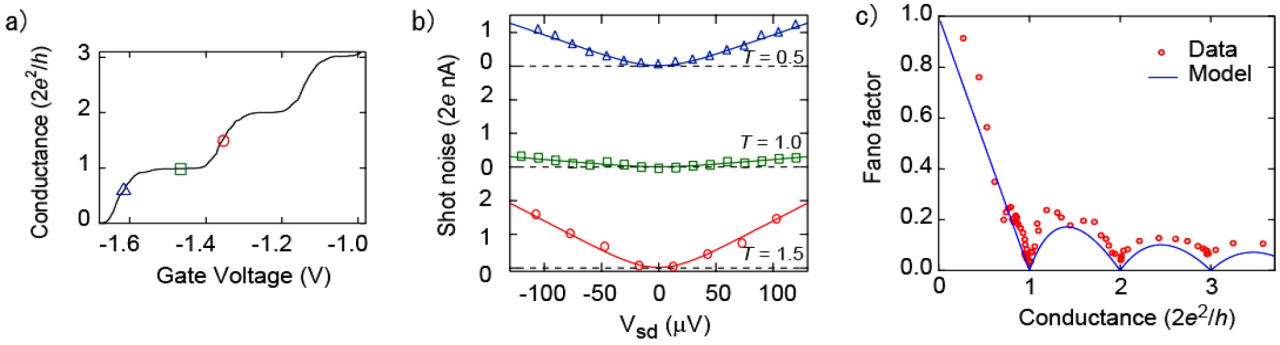

Fig. 8.21 Shot noise measured on a quantized conductance plateau of a QPC, and at around transition regions. (a) QPC conductance as a function of the gate voltage. Positions for noise measurements are indicated by color-framed open symbols. (b) Shoit noise measured at the three points indicated in (a) as a function of the source-drain voltage. (c) Fano factor (red circles) as a function of the conductance of the QPC. The blue line is obtained from a simple model, in which Fano factor should be $1 - \mathcal{T}$. From [6].

Figure 8.21 shows an example of shot noise measurement of a QPC. In panel (a), the conductance is shown as a function of the gate voltage and the current noise (spectral density of the square of current fluctuation) were measured at the three points indicated by color-framed symbols (on a conductance plateau and at neighboring transition regions). In panel (b), the current noise is plotted versus the source-drain voltage. In the transient regions, the noise increases with the voltage indicating the appearance of shot noise while around the center of plateau, the increase of noise is very small, indicating the reduction of noise. In panel (c), the noise data are converted to Fano factor and shown as a function of the conductance. The blue line shows the consequence of a simple model, in which the Fano factor should be $1 - \mathcal{T}$. The data distribute a bit above the model line confirming the noise reduction with the conductance quantization.

8.6.2 Transport of exciton-polaritons

As a bosonic quasiparticle, we consider exciton-polariton (E-P), which is introduced in Sec. 4.4.2. An E-P is a composite of photons and excitons created as a result of strong coupling of light and matter. Being pairs of fermions, excitons obey Bose statistics but the effective mass is the sum of those for electrons and holes as $m_e + m_h$. On the other hand, as can be seen from the dispersion relation in Fig. 4.7, an E-P has a very small effective mass around $k \approx 0$. This makes the control of phase of E-Ps easier and the reseachers are trying to apply E-Ps for optical integrated circuits. The light effective mass makes the critical temperature of BEC (8B.10) very high. Actually, the observations of BEC have been reported.

8.6.2.1 Cavity exciton-polariton

In the section of laser diode, we have seen a structure of two-dimensional cavity. In Fig. 8.22(a) we show a transmission line made by cutting the two-dimensional cavity into a thin mesa structure. Here, the structure is such that GaAs is used as a quantum well, which is sandwiched between GaAs / AlGaAs superlattices (SL), and a GaAs clad layer is placed on the outside. The effective refractive index of the SL part is lower than that of GaAs, and photons are confined in this region. On the other hand, excitons are confined in the central GaAs quantum well because the SL regions work as barriers due to the band discontinuity. The excitons in this case are confined in the two-dimensional plane of the cavity and as we saw in Sec. 7.1.3 the binding energy of the excitons becomes larger and they are stabilized. With the above devicing, E-Ps can propagate the waveguide but for stable propagation, we need to prepare some low temperature environments. The limit of temperature is extimated from the gap between the upper and the lower branches in the dispersion relation in Fig. 8.22(c) and that can be go over the liquid nitrogen temperature.

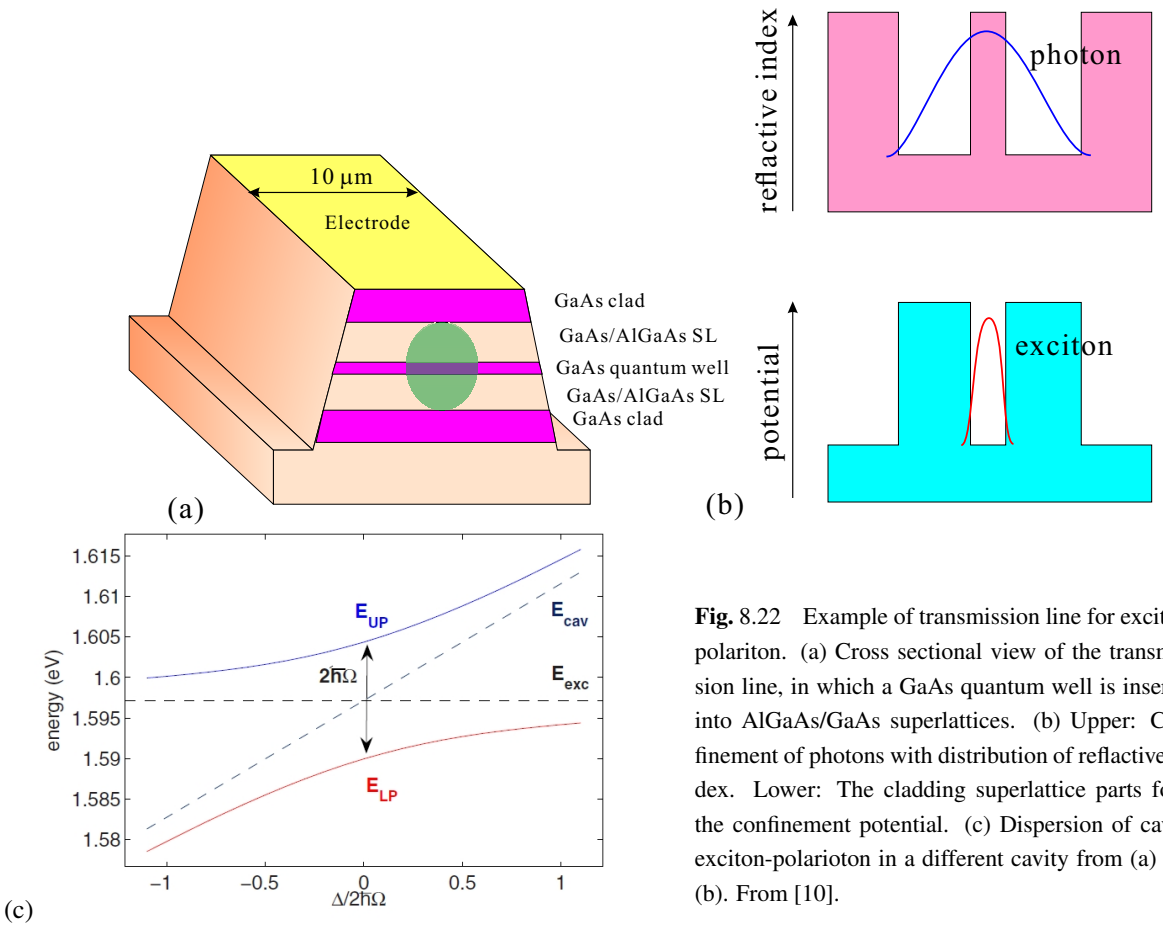

Fig. 8.22 Example of transmission line for exciton-polariton. (a) Cross sectional view of the transmission line, in which a GaAs quantum well is inserted into AlGaAs/GaAs superlattices. (b) Upper: Confinement of photons with distribution of reflactive index. Lower: The cladding superlattice parts form the confinement potential. (c) Dispersion of cavity exciton-polarioton in a different cavity from (a) and (b). From [10].

The dispersion relation in Fig. 4.7 is made up from photons in crystals and excitons. In the present E-P waveguide, the photons are strongly confined into the micro-cavity and the photon dispersion relation changed from that in bulk. Figure 8.22(c) shows the avoided crossing between the cavity photon and the exciton caused by the strong coupling of light and matter. The structure of cavity here for the calculation of the dispersion is shown in Fig. 8.24.

In the left panel of Fig. 8.23, a conceptual figure of a Mach-Zehnder (MZ)-type interference device composed of the cavity transmission line shown in Fig. 8.22(a). As mentioned in the section of exciton, because the response to the electric field is opposite for electrons and holes, if is is a comletely single-body composite particle, the effect of the electric field can be hardly observied. However, in the structure of Fig. 8.22(a), the binding energy of excitons can be varied by the electric field and with that, the wavenumber varies as

$$\Delta\varphi = L\left[\frac{\sqrt{2mE_k}}{\hbar} - \frac{\sqrt{2m(E_k - \delta E)}}{\hbar}\right]. \tag{8.58}$$

δE represents this variation in the kinetic energy and L is the length of the gate region. This gives modulation in the output of the two-path circuit shown in the left panel of Fig. 8.23. Finally the output is transposed into light at the edge of the transmission line and the output can be detected as the light strength. The transmission circuit in Fig. 8.23 is called in the paper[7], as an MZ interferometer though, because it has a single output line, some reflection exists at the joint, it should be called as a two-path AB-type (in the present case, the AB phase does not exist and "ring-type" may be a better expression). As shown in Fig. 8.23(a), (b), with the voltage the light ouput power can be controlled by over 10 dB and voltage-light switching function is realized.

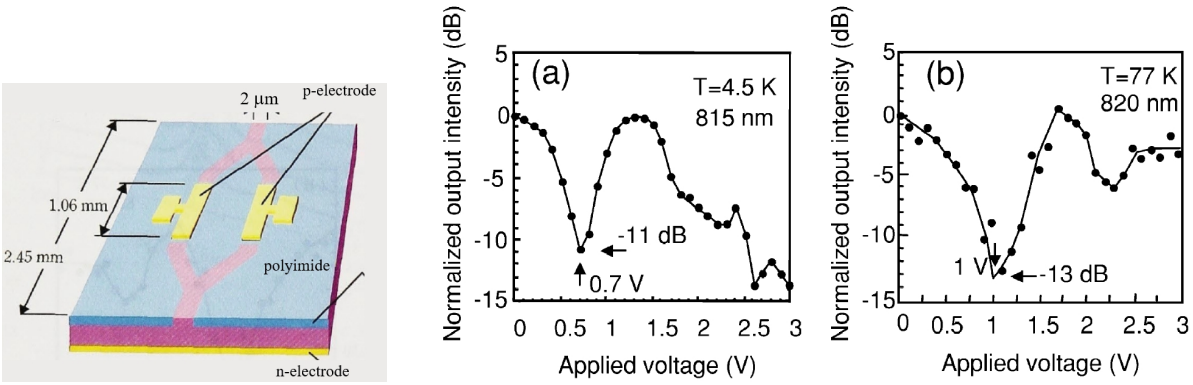

Fig. 8.23 Left panel: Concept of Mach-Zehnder (MZ)-type interference device. (a) Variation in the ouput of MZ interference device versus gate voltage (4.5 K). (b) The same for 77 K.

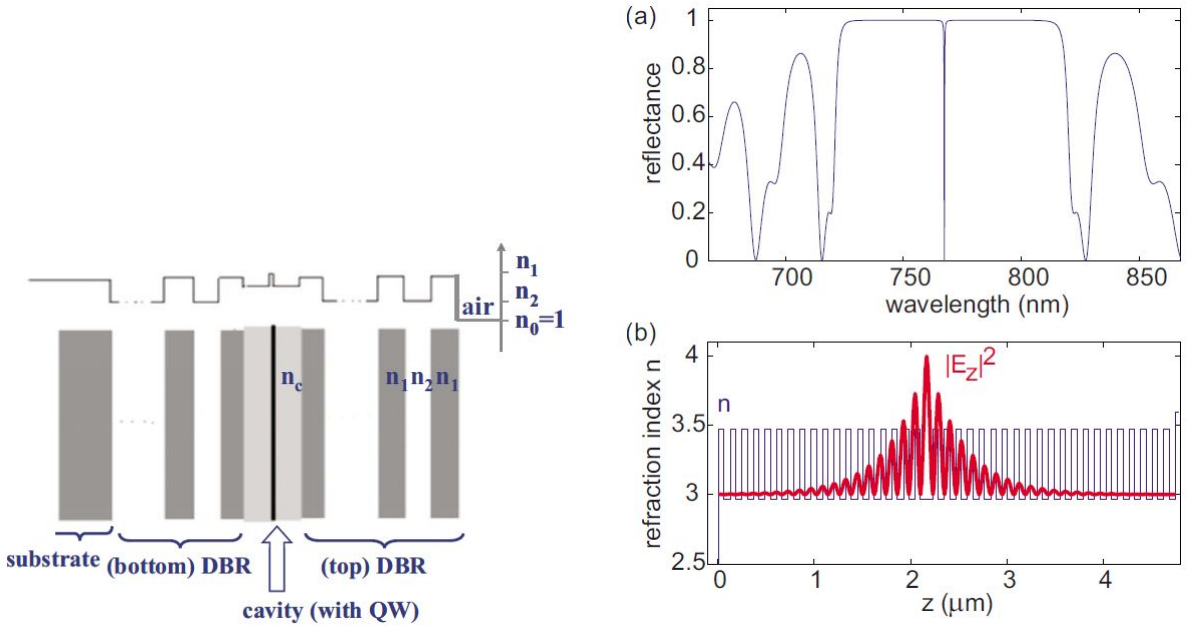

Fig. 8.24 Left panel: Schematic view of the cavity transmission line for the observation of exciton-polariton condensation. Upper figure shows the refractive index. Right panel: (a) Calculated reflection coefficient of hte left cavity. (b) Structure of reflactive index in the cavity. The red line is the distribution of electric field along z-axis for the localized mode showing the sharp resonant dip around the center of the spectrum shown in (a). From [10].

8.6.2.2 Condensation of exciton-polariton

While electrons are the representative of fermions flowing through quantum circuits, as we have seen above, E-Ps in microcavities is a system, with which we can explore the boson flow through quantum circuits experimentally. The consequence of Fermi statistics on fermion flow in quantum circuits is the conductance quantization and the reduction of shot noise. On the other hand, bunching of the identical particles is the characteristics of the Bose statistics, as we have seen in Sec. 8.6.1. As a result, **Bose-Einstein condensation** (BEC) or similar phenomenon with condensation occurs. The stimulated emission is also a phenomenon similar to the boson bunching, and photons in a cavity of a laser can be viewed as a kind of condensation though the lasing occurs in non-equilibrium open systems while BEC is a phenomenon in equilibrium. There is thus a clear difference[8, 9].

Figure 8.24 shows the diagram of refractive index in the cavity prepared for the observation of BEC. This figure also

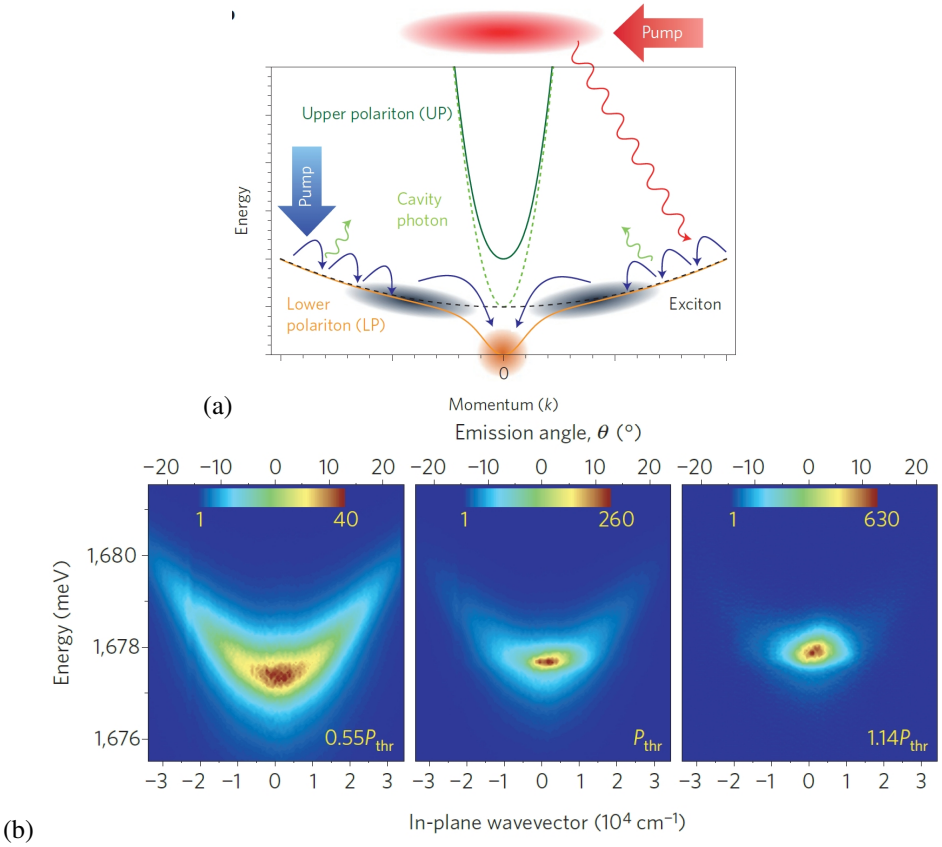

Fig. 8.25 (a) Conceptial diagram illustrating the "cooling" process for micro-cavity E-P to cause BEC. (b) Ditribution of E-Ps in the space of wavenumber and the energy measured from the optical emission. $P_{\rm th}$ is the critical excitation power to create E-Ps with the critical particle density for BEC. from [9].

shows the energy density of electric field along z-axis in the mode localized at the center of cavity, which is calculated with T-matrix method. T-matrice and S-matrices are thus used to calculate various quantities related to wave propagations.

A short summary on BEC of three dimensional ideal boson gas is given in Appendix 8B. As the expression of the critical temperature $T_{\rm c}$ in Eq. (8B.10), the lighter the effective mass is, and also the higher the particle density is, the higher $T_{\rm c}$ becomes. Conversely, when the mass and the temperature are given, the critical particle density for BEC to appear is defined.

Figure 8.25(a) illustrates the process of creation of a BEC with laser light irradiation on the cavity system. In the beginning of the process, many E-Ps with high energies are excited with the lase pulse. They emit energies as phonons to the crystal and are cooled down. If the laser power is higher than the critical value $P_{\rm th}$, as cooling, a BEC is created and a macroscopic number of E-Ps fall into the lowest energy state. In Fig. 8.25(b), the wavenumber-energy distributions of E-Ps measured from light leakage, are given around the BEC critical power.

Here we need to be careful about the meaning of "BEC." The present E-P system is composed of modes confined to a 2-dimensional plane and 3-dimensional BEC in App. 8B cannot be directly applied. In the space with dimension lower than or equal to 2, no infinitely long range order does not exist as mentioned in Mermin-Wagner theorem[11]. Instead, Berezinskii-Kosterlitz-Thouless (BKT) transition occurs and the order decays with some power of the distance[12]. Actually, the existence of BKT transition was evidenced in detailed analysis of experiments. And the observation of vortex-pair is announced. There are so many reports on the BEC of E-P systems and the research is active both in theory and experiment.

Appendix 7A: Laser diode and waveguide

Here a short supplement on the structure of waveguide for laser diode (LD) is given. Let us consider the Fabry-Pérot type LD with waveguide (cavity) length L. Let m_j, $\bar{n}$ and λ be an integer, the reflactive index, and the wavelength in the vacuum respectively, then the condition of resonance is

$$m_j \frac{\lambda}{\bar{n}} = 2L. \tag{7A.1}$$

Therefore the interval in the resonant wavelengths and that in the resonant frequencies are

$$\Delta\lambda = \frac{\lambda^2}{2L\bar{n}}, \quad \Delta\nu = \frac{c}{2L\bar{n}}, \tag{7A.2}$$

respectively. In usual systems, $\lambda \ll L$. When the amount of carrier injection is large and the luminescence is broad in wavelength, precise determination of l is not requied monstly and multi-mode oscillation around a center wavelenth is observed.

In the above, we write the light intensity simply as $I_0 \exp(-\alpha' z)$. Then α' can be expanded as $I(z) = I_0 \exp((g-\alpha)z)$, where g is the optical gain, α is the material specific absorption coefficient. Let us write the reflection ratio of the two mirrors as R_1 and R_2 respectivly, then the condition for the amplification to occur is

$$R_1 R_2 \exp[(g-\alpha)2L] > 1.$$

Thus the threshold optical gain $g_{\rm th}$ for the total amplification is

$$g_{\rm th} = \alpha + \frac{1}{L} \ln\left(\frac{1}{R_1 R_2}\right). \tag{7A.3}$$

The reflactive index $\bar{n}_1$ is common for both sides of the homo pn-junction, while the reflactive index in the active layer $\bar{n}_2$ is larger than $\bar{n}_1$. z-axis is taken as in the figure and we consider the electromagnetic wave propagate along the z-axis. The propagation mode is transverse electric (TE), i.e., the electric field along z axis is absent ($\mathcal{E}_z = 0$). Also the mode is assumed to be uniform in y direction. Thus we only need to consider the elecric field in y direction, which is determined from

$$\left[\frac{\partial^2}{\partial x^2} + \frac{\partial^2}{\partial z^2} - \mu_0 \epsilon_0 \epsilon \frac{\partial^2}{\partial t^2}\right] \mathcal{E}_y = 0. \tag{7A.4}$$

The change of magnetic permeability in semiconductors from the vacuum is little then we use μ_0 here.

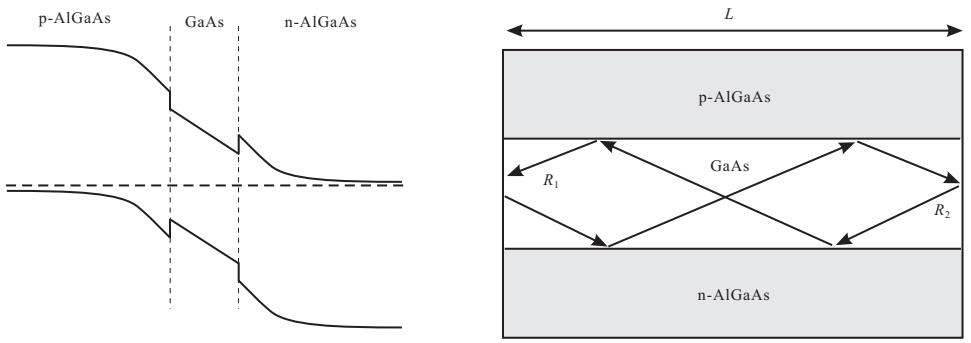

Fig. 7A.1 Left panel: Schematic band diagram of a pn-junction for LD. The active layer is non-doped GaAs and the doping layers with larger band gap than that of the active layer, are AlGaAs. Right panel: Substrate edges are formed by cleaving and work as half mirrors, which make the active GaAs layer into a cavity.

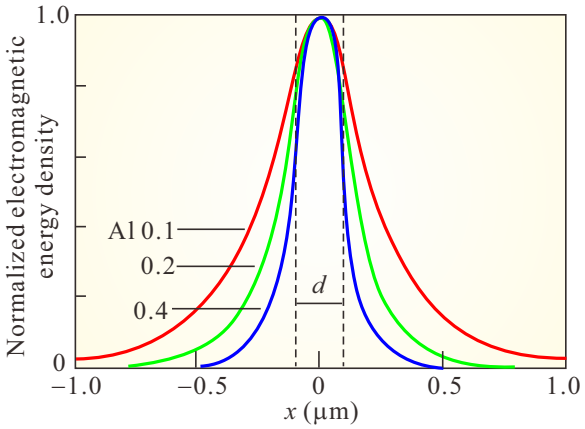

Fig. 7A.2 Distribution of normalized electromagnetic energy density of fundamental mode on x (origin at the center of active layer) in a cavity with an active (i-)layer of GaAs, The parameter is the content of Al.

We treat the system as a waveguide and look for a solution of standing wave on x and propagating wave on z. Then we find a solution inside the active layer ($|x| \leq d/2$) as

$$\mathcal{E}_y(x,z,t) = A\cos(\kappa x)\exp[i(\omega t - \beta z)], \tag{7A.5}$$

where

$$\kappa^2 = \mu_0\epsilon\epsilon_0\omega^2 - \beta^2 = \bar{n}_2^2 k_0^2 - \beta^2, \quad k_0 = \frac{\omega}{c^*\bar{n}_2}. \tag{7A.6}$$

And outside the active layer ($|x| > d/2$), the solution should decay with $|x| \to \infty$. The condition of connection at $x = \pm d/2$ での $\mathcal{E}_y$ restricts the solution to

$$\mathcal{E}_y(x,z,t) = A\cos\left(\frac{\kappa d}{2}\right)\exp\left[-\gamma\left(|x| - \frac{d}{2}\right)\right]\exp[i(\omega t - \beta z)]. \tag{7A.7}$$

Equation (7A.4) requires

$$\gamma^2 = \beta^2 - \bar{n}_1^2 k_0^2. \tag{7A.8}$$

From Maxwell equation, the continuity in z-component of magnetic field at $x = \pm d/2$ requires

$$\tan\left(\frac{\kappa d}{2}\right) = \frac{\gamma}{\kappa} = \frac{\sqrt{\beta^2 - \bar{n}_1^2 k_0^2}}{\sqrt{\bar{n}_2^2 k_0^2 - \beta^2}}. \tag{7A.9}$$

The values of κ, γ and β are determined from the above equations. Because tangent is a π-periodic function, there are multiple solutions, each of which forms a descrete mode.

Appendix 8A: Shot noise

We express information as a time-varying physical quantity and transmit it using various transport phenomena. Every physical quantity has fluctuations and among them time varing ones are called **noise** [*3]. The noise can be classified into external noise and **intrinsic noise**. While the former comes from "outside" of the system, the latter is included in the physics of the quantity itself. Particularly in the case of electric current by electron flow, the representative intrinsic noises are thermal noise (Johnson-Nyquist noise) that caused by random thermal motion of electrons and **shot noise** that originates from the particle nature of electrons and the randomness in the flow.

Let us consider first the current by a single electron observed at time t_p, expressed as $J_p(t) = e\delta(t - t_p)$. From the Fourier expansion

$$J_p(t) = e\int_{-\infty}^{\infty}\exp[2\pi i f(t-t_p)]df = 2e\int_0^{\infty}\cos[2\pi f(t-t_p)]df, \tag{8A.1}$$

[*3] Fluctuation means the distribution of observed values in multiple identical measurements and the parameter of sampling is not restricted to time. An example of non-time dependent fluctuation is aperiodic conductance oscillations in disordered mesoscopic conductors(P. A. Lee and A. D. Stone, Phys. Rev. Lett. **55**, 1622 (1985)).

we see that the current itself has an amplitude of $2e$ independent of frequency. In the infinitesimal frequency width df at frequency f, we take the average $\langle \cdots \rangle$ over one period. Let us write the integrand in (8A.1) as j_p and the current flusctuation is $\delta J_p = \sqrt{\langle j_p^2 \rangle} df = \sqrt{2} e df$.

Next we consider an electric current by two electrons observed at t_p and t_q, $J_{pq} = e[\delta(t - t_p) + \delta(t - t_q)]$. In the Fourier transform of J_{pq}, there is a phase difference $\phi = f(t_q - t_p)$ between the two Fourier components from the two delta-functions. The phase difference appears in the square of Fourier transformed function as an interference term:

$$j_{pq}^2 = j_p^2 + j_q^2 + 2 j_p j_q \cos\phi. \tag{8A.2}$$

The interference terms, however, cancel out when we add up many such two-electron currents and take the average (represented as $\overline{\cdots}$ due to the randomness in $t_q - t_p$, i.e. $\overline{j_{pq}^2} = 2(\sqrt{2}e)^2$. A current by many electrons randomized on time is equivalent to this many sampling. Hence, let N be the time averaged number of flowing electrons then the averaged current is $J = eN$ and the current fluctuation over the bandwidth Δf is

$$\langle (\delta J)^2 \rangle / \Delta f (\equiv S_{\text{Poisson}}) = N \times 2e^2 = 2eJ. \tag{8A.3}$$

The square of current fluctuation is proportional to the average of current corresponds to the fact the variance of Poisson distribution is the average (the number of electrons per unit time N). This case of complete randomness is called **Poisson noise**.

On the other hand, when the electrons flow with a constant interval, there is no fluctuation(timing of sampling would result in shifts of e in counted charge, but this is not a random variation). This can be understood from Fourier analysis of the current. Let us write the regular series of delta function with interval as τ as $\delta_\tau(t)$. Because $\delta_\tau(t)$ is a τ-periodic function, the Fourier series expansion on the region $[-\pi/\tau, \pi/\tau]$ is possible as follows.

$$\delta_\tau(t) = \frac{1}{\tau} \sum_{n=-\infty}^{\infty} \exp\left(-in\frac{2\pi}{\tau}t\right). \tag{8A.4}$$

Then the Fourier transform is written as

$$\begin{aligned} \mathscr{F}\{\delta_\tau(t)\} = \int_{-\infty}^{\infty} \left[\frac{1}{\tau}\sum_{-\infty}^{\infty} e^{-in(2\pi/\tau)t}\right] e^{i\omega t} dt &= \frac{1}{\tau}\sum_{n=-\infty}^{\infty} \int_{-\infty}^{\infty} \exp\left[i\left(\omega - n\frac{2\pi}{\tau}\right)t\right] dt \\ &= \frac{2\pi}{\tau}\sum_{n=-\infty}^{\infty} \delta\left(\omega - n\frac{2\pi}{\tau}\right) = \frac{2\pi}{\tau}\delta_{2\pi/\tau}(\omega), \end{aligned} \tag{8A.5}$$

that is, it is also a regular series in ω space and there is no continnum spectrum, which is the sign of random variation. This means the disappearance of shot noise.

Appendix 8B: Bose-Einstein condensation

The Bose-Einstein Condensation (BEC) [*4] is called a phase transitoin that is not due to the interaction between freedoms (quantum statistical phase transition). Though phase transitions caused by interaction beween some freedoms can be intuitively understood, there are different types of phase transitions, in which the transitions are caused as the results of competition between various factors. A representative is BEC.

In the case of bosonic systems, in spite of the absence of "force" betwen the particles, there exists the tendency for them to occupy the same quantum state originating from their statistical property. Let us see that for the case of two

[*4] The acronym of BEC is applied to both Bose-Einstein Condensation and Bose-Einstein Condensate. In actual use, the confution is not serious.

particles. We write a solution of the wave equation for two particles as $\psi(\boldsymbol{x}_1, \boldsymbol{x}_2)$. For the composition of wavefunctions of the system $\Psi(\boldsymbol{x}_1, \boldsymbol{x}_2)$ that reflects the statistical property of bosons, the symmetrization of ψ results in

$$\Psi(\boldsymbol{x}_1, \boldsymbol{x}_2) = \frac{1}{\sqrt{2}} \left[\psi(\boldsymbol{x}_1, \boldsymbol{x}_2) + \psi(\boldsymbol{x}_2, \boldsymbol{x}_1)\right]. \tag{8B.1}$$

Hence the probability of finding the system at $(\boldsymbol{x}_1, \boldsymbol{x}_2)$ is

$$|\Psi(\boldsymbol{x}_1, \boldsymbol{x}_2)|^2 = \frac{1}{2} \left[|\psi(\boldsymbol{x}_1, \boldsymbol{x}_2)|^2 + |\psi(\boldsymbol{x}_2, \boldsymbol{x}_1)|^2 + \psi(\boldsymbol{x}_1, \boldsymbol{x}_2)^* \psi(\boldsymbol{x}_2, \boldsymbol{x}_1) + \psi(\boldsymbol{x}_1, \boldsymbol{x}_2) \psi(\boldsymbol{x}_2, \boldsymbol{x}_1)^*\right]. \tag{8B.2}$$

This reveals that the last two interference terms intensify the probability of finding the system under the condition of $\boldsymbol{x}_1 = \boldsymbol{x}_2$. Let us write the de Broglie wavelength as λ and the averaged distance between the particles as l. Then at low temperatures $\lambda \sim l$, this tendency of bosons makes many of them to occupy the state of $k = 0$, which behavior leads to BEC. The above discusstion is expressed as

$$E_k = \frac{p^2}{2M} = k_{\mathrm{B}} T,$$

$$\begin{aligned} &\Delta p \sim \sqrt{M k_{\mathrm{B}} T} \\ &\therefore \lambda = \frac{h}{\Delta p} \sim \frac{h}{\sqrt{M k_{\mathrm{B}} T}}. \end{aligned} \tag{8B.3}$$

λ elongates as $1/\sqrt{T}$ with lowering the temperature. And with growing of the overlapp between the single particle wavefunctions makes them undistinguishable and the symmetrization of the wavefunction cause the condensation to the ground state in the phase space $(\boldsymbol{r}, \boldsymbol{p})$. The phase transition to the condensate at a certain temperature is BEC.

8B.1 Bose-Einstein condensation of ideal gas

Let us consider spin 0 ideal Bose gas. For the Bose distribution

$$f(\epsilon) = \frac{1}{e^{(\epsilon - \mu)\beta} - 1} \qquad (\beta \equiv (k_{\mathrm{B}} T)^{-1}) \tag{8B.4}$$

we define the point of $\mu = 0$ as follows. At $T = 0$, from (8B.4) all the particles fall into the ground state, there we define

$$\mu(T = 0) = 0. \tag{8B.5}$$

At finite temperatures, let N be the number of particles in the system:

$$N = \sum_i f(\epsilon_i).$$

In the usual case we can write

$$N \to \int f(\epsilon) \mathcal{D}(\epsilon) d\epsilon. \tag{?}$$

Here the number of particle at the ground state N_0 should be

$$N_0 = \frac{1}{e^{-\mu\beta} - 1} \sim \frac{1}{-\mu\beta} = -\frac{k_{\mathrm{B}} T}{\mu} \to \mu \sim -\frac{k_{\mathrm{B}} T}{N_0}. \tag{8B.6}$$

If we calculate the particle distribution on this line, for three dimensional ideal gas

$$\epsilon(k) = \frac{\hbar^2 k^2}{2m} \quad \text{then} \quad \mathcal{D}(\epsilon) = \frac{m^{3/2} V}{\sqrt{2} \pi^2 \hbar^3} \sqrt{\epsilon}. \tag{8B.7}$$

Therefore

$$N = \frac{V m^{3/2}}{\sqrt{2} \pi^2 \hbar^3} \int_0^\infty \frac{\sqrt{\epsilon}}{e^{(\epsilon - \mu)\beta} - 1} d\epsilon = \frac{(m k_{\mathrm{B}} T)^{3/2}}{\sqrt{2} \pi^2 \hbar^3} V \int_0^\infty \frac{\sqrt{x}}{e^{x - \alpha} - 1} dx, \tag{8B.8}$$

where $x \equiv \epsilon\beta$ and $\alpha \equiv \mu\beta$. We write the definite integral term as $I(\alpha)$, then I is

$$I(0) = \int_0^\infty \frac{\sqrt{x}}{e^x - 1} dx = \frac{\sqrt{\pi}}{2} \zeta\left(\frac{3}{2}\right) \sim 2.6, \tag{8B.9}$$

which decreases with increasing of the absolute value of $\alpha < 0$. Then, in this logic, with $T \to 0$ the maximum number of N determined from (8B.8) goes to zeo. It is apparent that we have dropped something from the counting. That is, of course, the macroscopic number of particles fall into the ground state.

From Eq. (8B.8),

$$I(\alpha) = \frac{\sqrt{2}\pi^2\hbar^3}{(mk_{\mathrm{B}}T)^{3/2}} \frac{N}{V}.$$

When this excessds (8B.9) at low temperatures the anomaly (increase in the particle number at the ground state.) occurs. This critical temperature T_c is

$$T < T_c \equiv \frac{2\pi\hbar^2}{mk_{\mathrm{B}}} \left[\frac{N}{\zeta(3/2)V}\right]^{2/3}. \tag{8B.10}$$

Here $l \equiv (V/N)^{1/3}$ is the average distance between the particles and Eq. (8B.10) is interpreted as

$$l = \frac{h}{\zeta(3/2)\sqrt{2\pi m k_{\mathrm{B}} T_c}} \sim \lambda(T = T_c). \tag{8B.11}$$

This confirms the statement that the BEC takes place when the average de Broglie wavelength is comparable with the average particel distance.

Below T_c, we add the number of ground state particles N_0 to Eq. (8B.8):

$$N = \frac{Vm^{3/2}}{\sqrt{2}\pi^2\hbar^3} \int_0^\infty \frac{\sqrt{\epsilon}}{e^{(\epsilon-\mu)\beta} - 1} d\epsilon + N_0. \tag{8B.12}$$

From Eq. (8B.6), N_0 becomes a macroscopic number fro $T < T_c$, then $\mu = 0$. Therefore

$$N_0 = N - \frac{Vm^{3/2}}{\sqrt{2}\pi^2\hbar^3} \int_0^\infty \frac{\sqrt{\epsilon}}{e^{\epsilon\beta} - 1} d\epsilon = N\left[1 - \frac{V}{N}\frac{(mk_{\mathrm{B}}T)^{3/2}}{\sqrt{2}\pi^2\hbar^3} I(0)\right] = N\left[1 - \left(\frac{T}{T_c}\right)^{3/2}\right]. \tag{8B.13}$$

This is just like a spontaneous magnetization rapidly grows to finite values below the critical temperature in the ferromagnetic transition.

The total energy of the system for $T < T_c$ is calculated as

$$E = \frac{Vm^{3/2}}{\sqrt{2}\pi^2\hbar^3} \int_0^\infty \frac{\epsilon^{3/2}}{e^{\beta\epsilon} - 1} d\epsilon \tag{8B.14}$$

ここで $T < T_c$ では $\displaystyle\int_0^\infty \frac{x^{3/2}}{e^x - 1} dx = \frac{3\sqrt{\pi}}{4} \zeta\left(\frac{5}{2}\right)$ より

$$E = \frac{3}{2}\zeta\left(\frac{5}{2}\right)\left(\frac{m}{2\pi\hbar^2}\right)^{3/2} V(k_{\mathrm{B}}T)^{5/2}. \tag{8B.15}$$

Then the heat capacity at constant volume is calculated as

$$C_v = \frac{15}{4}\zeta\left(\frac{5}{2}\right)\left(\frac{m}{2\pi\hbar^2}\right)^{3/2} V k_{\mathrm{B}}^{5/2} T^{3/2}. \tag{8B.16}$$

C_v shows a cusp at T_c indicating that this is the phase transition.

8B.2 Bosonic stimulation

Here we have a look at **bosonic stimulation** for N particles, which is, though, essentially the same as what has been mentioned on the case of two particles in Sed. 8.6.1. As we have seen, the bosonic stimulation works as if it is a driving

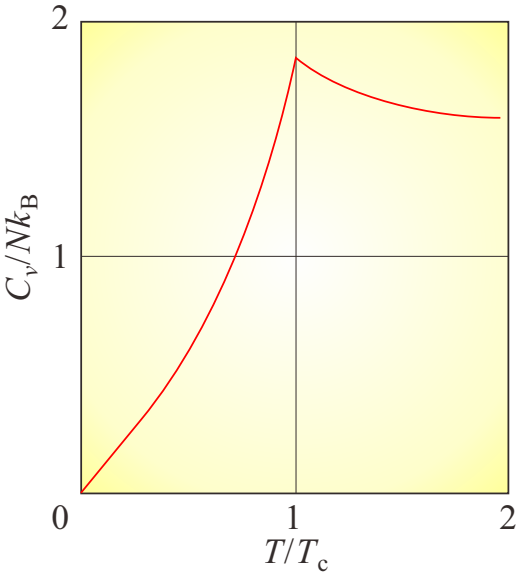

Fig. 8B.1 Specific heat at constant volume of three dimensional ideal Bose gas as a function of temperature. T_c is the critical temperature of the BEC.

force in BEC or laser oscillation. Let us consider a identical boson system the case a particle in state $\varphi_{\rm ini}$ gets perturbation and transitions to other single particel state $\varphi_{\rm fin}$. Now the problem is the difference in the transition probabilities to the state occupied with N particles and to the empty state. We write the initial state as

$$\psi_+^{(i)}(\boldsymbol{r}_1,\cdots,\boldsymbol{r}_{N+1}) = \frac{1}{\sqrt{(N+1)N!\prod_l n_l!}} \prod_{m=1}^{N} \hat{R}_{m,N+1} \det{}^{(+)}\{\varphi_i(\boldsymbol{r}_j)\}\varphi_{\rm ini}(\boldsymbol{r}_{N+1}). \tag{8B.17}$$

The symbol $\det^{(+)}$ represents permanent, which is obtained by making the signs of all the terms into $+$. The final state $\psi_+^{(f)}$ is obtaned by exchanging $\varphi_{\rm ini}$ with $\varphi_{\rm fin}$. Let the matrix elements of perturbation Hamiltonian be a, i.e. $\langle\varphi_{\rm fin}|\hat{H}_1|\varphi_{\rm ini}\rangle = a$.

Assuming that φ_i $(i \le N)$ is orthogonal to $\varphi_{\rm fin}$, among $\langle\psi_+^{(f)}|\hat{H}_1|\psi_+^{(i)}\rangle$, number of terms that give non-zero a is $(N+1)N!\prod_l n_l!$. This is equal to the sqare of the denominator in normalization constant. Then finally $\langle\psi_+^{(f)}|\hat{H}_1|\psi_+^{(i)}\rangle = a$.

On the other hand, assuming all of φ_i $(i \le N)$ are $\varphi_{\rm fin}$, we can write

$$\psi_+^{(i)} = \frac{1}{\sqrt{(N+1)}} \prod_{m=1}^{N} \hat{R}_{m,N+1}\varphi_{\rm fin}(\boldsymbol{r}_1)\cdots\varphi_{\rm fin}(\boldsymbol{r}_N)\varphi_{\rm ini}(\boldsymbol{r}_{N+1}). \tag{8B.18}$$

All of the $N!$ terms in $\det^{(+)}$ are $\varphi_{\rm fin}(\boldsymbol{r}_1)\cdots\varphi_{\rm fin}(\boldsymbol{r}_N)$ and devided by $N!$ in the denominator of normalization constant to 1. However the final state is

$$\psi_+^{(f)} = \varphi_{\rm fin}(\boldsymbol{r}_1)\cdots\varphi_{\rm fin}(\boldsymbol{r}_N)\varphi_{\rm fin}(\boldsymbol{r}_{N+1}). \tag{8B.19}$$

Then we get $\langle\varphi_{\rm fin}|\hat{H}_1|\varphi_{\rm ini}\rangle = a\sqrt{N+1}$, and from the Fermi's golden rule, the transition probability should be $N+1$ times larger.

References

[1] S. Datta, "ElectronTransport in Mesoscopic Systems" (Cambridge Univ. Press, 1995).

[2] 勝本信吾 「メゾスコピック系」 (朝倉書店，2002)

[3] Y. Gefen, Y. Imry, and M. Ya. Azbel, Phys. Rev. Lett. **52**, 129 (1984).

[4] A. Yacoby, R. Schuster, and M. Heiblum, Phys. Rev. B **53**, 9583 (1996).
[5] A. Aharony, O. Entin-Wohlman, T. Otsuka, H. Aikawa, S. Katsumoto and K. Kobayashi, Phys. Rev. B **73**, 195329 (2006).
[6] M. Hashisaka, Y. Yamauchi, S. Nakamura, S. Kasai, K. Kobayashi, and T. Ono, J. Phys.: Conf. Ser. **109**, 012013 (2008).
[7] K. Ogawa, T. Katsuyama and H. Nakamura, Phys. Rev. Lett. **64**, 796 (1990).
[8] 山本喜久，宇都宮聖子，日本物理学会誌 **67**, 96 (2012).
[9] T. Byrnes, N.-Y. Kim, and Y. Yamamoto, Nat. Phys. **10**, 803 (2014).
[10] H. Deng, H. Haug, and Y. Yamamoto, Rev. Mod. Phys. **82**, 1489 (2010).
[11] N. D. Mermin and H. Wagner, Phys. Rev. Lett. **17**, 1133 (1966).
[12] P. Minnhagen, Rev. Mos. Phys. **59**, 1001 (1987).